Journal of Alloys and Compounds 489 (2010) 237–241

Contents lists available at ScienceDirect

Journal of Alloys and Compounds

journal homepage: www.elsevier.com/locate/jallcom

Oxidation behavior, microstructure evolution and thermal stability in nanostructured CrN/AlN multilayer hard coatings

Shih-Kang Tien, Chih-Hsiung Lin, Yan-Zuo Tsai, Jenq-Gong Duh*

Department of Materials Science and Engineering, National Tsing Hua University, Hsinchu 30013, Taiwan

ARTICLE INFO

Article history:
Received 23 August 2009
Accepted 12 September 2009
Available online 19 September 2009

Keywords:
CrN/AlN
TEM
Oxidation behavior
Nano-crystalline
RF sputtering
Multilayer coating

ABSTRACT

CrN/AlN multilayer coatings with modulation period of 4 and 12.3 nm were manufactured by RF magnetron sputtering. The films were annealed at temperatures 800–950 °C for 1 h in air environment. The microstructure evolution and chemical composition of the formed oxides after heat treatment were identified by transmission electron microscope (TEM) and energy dispersive spectrometer (EDS). After heat treatment at 800 °C for 1 h, three regions which formed on the surface of CrN/AlN coatings with 12.3 nm modulation was observed, including the Al-rich layer covered at the topmost surface, the mixed nano-crystalline Al_2O_3 and Cr_2O_3 film and the spherical nano-voids embedded in between. On the contrary, for CrN/AlN coating with a modulation period of 4 nm, the dense oxide layer around 37 nm formed on the top of the un-reacted film was much thinner than that of CrN/AlN coating with 12.3 nm. Besides, no nano-voids was detected which implied that the outward diffusion of atom species was suppressed as compared to that in the film with 12.3 nm. The presence of the topmost Al-rich layer protected the multilayer coating from the outward diffusion of Cr and Al, as well as the inward diffusion of oxygen. After 950 °C for 1 h and 800 °C for 16 h, the grain growth of surface oxides occurred and non-uniform interface between oxide and coating was also determined by TEM in the CrN/AlN multilayer coating with 12.3 nm. However, no substantial oxidations were detected in the coating with modulation period of 4 nm. It was evident that the CrN/AlN multilayer with smaller modulation period exhibited better oxidation resistance.

1. Introduction

Multilayer nitride coatings consisted of two different material assemblies and specific interface exhibit excellent mechanical performances, such as hardness, wear resistance and oxidation resistance [1–7]. Recently, studies have been mainly focused on the thermal reliability and oxidation resistance at elevated temperatures owing to the concerns about the inter-diffusion between two layers within the nano-meter scale and oxygen attacks [8–13]. These factors cast great influences on the mechanical strength and surface characteristics of the multilayer coatings. Barshilia et al. proposed that the decrease in hardness for TiN/CrN coating after heat treatment in air was caused by both the substantial oxidation on the surface and inter-diffusion at the interfaces [14]. In the ternary nitride systems, it was found that the Al dissolved nitride coating revealed excellent oxidation resistance, especially for CrAlN coating. Chromium aluminum nitride which exhibited better hardness and anti-oxidation resistance in comparison with the well-developed titanium aluminum nitride has been investigated [15]. Besides, the CrN/AlN multilayer coating was also proposed to further enhance the mechanical properties [16–18]. It was recently reported that the hardness of the CrN/AlN multilayer coating at elevated temperatures could be maintained, owing to the formation of the dense Al_2O_3 and Cr_2O_3 on the surface confirmed by XRD [17,18]. In spite of the enormous developments, the detailed microstructure and composition evaluation concerning the dense oxide formed on the surface at different temperatures in air environment were limited in literature.

This study was aimed to further investigate the detailed microstructure evolutions and chemical compositions of the oxides formed in the CrN/AlN multilayer coatings with different modulation periods at various temperatures ranged from 800 to 950 °C with the aid of electron microscopy characterization.

2. Experimental

CrN/AlN multilayer coatings were fabricated on the silicon (1 0 0) substrates by RF magnetron sputtering. The chromium and aluminum targets with 50.8 mm in diameter were 99.95 wt.% in purity. After loading substrates and targets, the deposition chamber was evacuated down to 8.0×10^{-4} Pa. The substrate temperature and rotation speed were controlled at 300 °C and 20 rpm, respectively, during deposition. The working distance for both sputtering guns was 60.0 mm. The target power was 150 W for Cr and 100 W for Al. The interlayer Cr with 40 nm was firstly coated on the Si substrate to enhance the adhesion between substrate and nitride coatings

* Corresponding author. Fax: +886 3 5712686.
E-mail address: jgd@mx.nthu.edu.tw (J.-G. Duh).

0925-8388/$ – see front matter © 2009 Elsevier B.V. All rights reserved.
doi:10.1016/j.jallcom.2009.09.060

by Ar incorporation as a plasma source. Then, the multilayer CrN/AlN coatings were fabricated and thickness of each layer was determined by the switch time of alternate shutters, which were controlled by a programmable logic control (PLC) after further introducing the nitrogen gas as the reaction sources to a working pressure of 2.0×10^{-1} Pa.

After deposition, the CrN/AlN multilayer coatings with 4 and 12.3 nm were annealed with a heating rate of 10 °C/min from room temperature to 800 °C for 1, 4 and 16 h and 950 °C for 1 h. The depth profile for elemental distributions of Cr, Al, O, and N were detected by Auger electron spectrometer combined with sputtering gun (AES, Auger NanoProbe, 670 PHI Xi, PerkinElmer, USA). The microstructure and modulation period of the CrN/AlN coatings after heat treatment were observed by transmission electron microscopy (JSM-2010, JEOL, Japan). For the TEM analysis, the samples were prepared by focus ion beam technique (FIB). The detailed phase and chemical composition were then analyzed by TEM equipped with EDS.

3. Results and discussion

3.1. Elemental distributions of the CrN/AlN multilayer coating

AES depth profile analysis of the CrN/AlN multilayer coating after heat treatment at 800 °C for 1 h is demonstrated in Fig. 1. The Al concentration was substantially accumulated on the surface as compared to that in the multilayer film, indicating that Al atom diffused outward owing to the attraction of oxygen. In order to realize the oxidation behavior of CrN/AlN multilayer coatings in air environment, the cross-sectional TEM equipped with EDS was used to observe the microstructure and composition of oxide film on the CrN/AlN multilayer coatings at elevated temperatures.

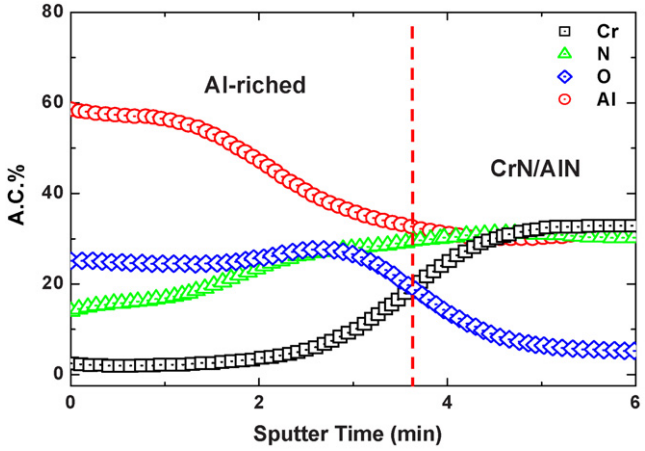

Fig. 1. AES depth profile of CrN/AlN multilayer coating with 12.3 nm after heat treatment at 800 °C for 1 h.

3.2. Microstructure analyses of the CrN/AlN multilayer coatings after heat treatment at 800 °C for 1 h

Fig. 2 shows the X'TEM image of CrN/AlN multilayer with 12.3 nm after heat treatment at 800 °C for 1 h. The bilayer structure of CrN/AlN multilayer was still present and displayed a sharp interface between two nitride layers. A thin oxide with thickness

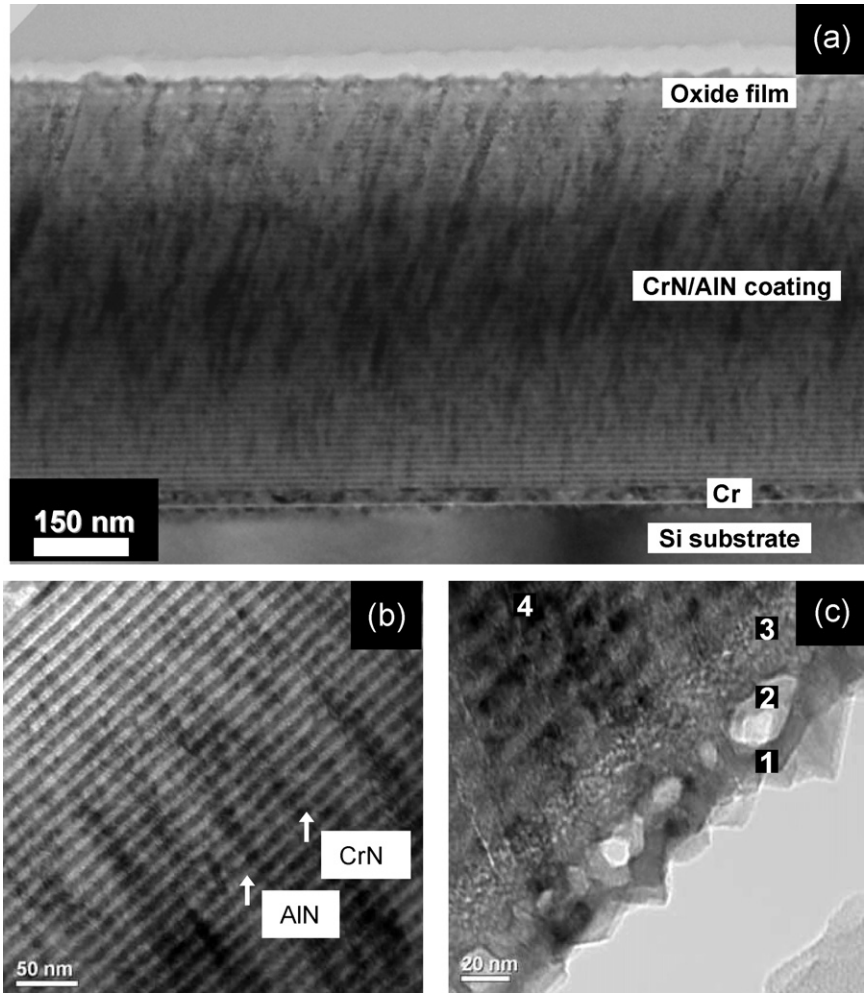

Fig. 2. (a) X'TEM image of CrN/AlN multilayer coating with 12.3 nm annealed at 800 °C for 1 h; (b) enlarged image of un-reacted film; and (c) enlarged image of oxide layer.

Table 1
Quantitative results of CrN/AlN multilayer coatings with 4 and 12.3 nm after heat treatment at 800, and 950 °C analyzed by TEM EDS.

Location[a]	Cr	Al	O	N	Phase
1	9.9	18.9	71.2	–	Crystalline Al-rich oxide
2	–	–	–	–	Nano-voids
3	17.6	16.3	66.2	–	Mixed $(Al_xCr_{1-x})_2O_3$
4	34.3	21.8	–	43.9	CrN/AlN film
5	5.8	27.4	66.8	–	Amorphous Al-rich oxide
6	25.0	14.3	60.7	–	Crystalline Cr-rich oxide
7	14.5	23.3	62.3	–	Mixed $(Al_xCr_{1-x})_2O_3$
8	8.7	25.4	65.9	–	Amorphous Al-rich oxide
9	14.9	22.5	62.6	–	Amorphous Al-rich oxide

[a] Points of analyzed location were indicated in Fig. 2 (points 1–4), Fig. 3 (point 5), Fig. 7 (points 6–7), and Fig. 8 (points 8–9).

around 60 nm was formed on the CrN/AlN multilayer coating. There existed three distinct regions in the oxide layer as identified in Fig. 2(c), including the crystalline phase at the outmost layer, a nano-crystalline film on the un-reacted CrN/AlN multilayer coating, and in between, the spherical nano-voids caused by the outward diffusion of atom species [19]. The compositions of both multilayer films and oxides quantitatively analyzed by TEM equipped with EDS are listed in Table 1. The outmost crystalline layer was Al-rich oxide, which was in agreement with the results of AES depth profile. The nano-crystalline layer was composed of mixed Cr_2O_3 and Al_2O_3 phases. According to the results obtained by TEM and AES depth profiles, when the CrN/AlN multilayer coatings were exposed to the air environment, AlN and CrN were oxidized simultaneously. Al then diffused outward to form the Al-rich oxide on the topmost surface, since thermodynamically the formation of Al_2O_3 was more stable as compared to that of Cr_2O_3 phase. Moreover, the activation energies for inward diffusions of O in Cr_2O_3 and Al_2O_3 were 424 and 460 kJ/mole, respectively, and those for diffusions of Cr in Cr_2O_3 and Al in Al_2O_3 were 255 and 477 kJ/mole, respectively [20,21]. It was reported that the oxidation of CrN film was mainly caused by the outward diffusion of Cr due to the lower activation energy of Cr in Cr_2O_3 (255 kJ/mole) [21]. As the Al-rich layer is formed on the topmost layer, it can impede the rapid Cr diffusion at elevated temperatures.

For CrN/AlN multilayer coating with 4 nm as shown in Fig. 3, the dense oxide layer around 37 nm formed on top of the un-reacted film was much thinner than that of CrN/AlN coating with 12.3 nm. The composition and structure of the topmost oxide layer analyzed by EDS revealed the presence of amorphous Al-rich $(Al_xCr_{1-x})_2O_3$ oxide (location 5 in Fig. 3). No any nano-void formations was observed between oxide layer and un-reacted film, which implied that the outward diffusion of atom species was suppressed as compared to that in the film with 12.3 nm. It was evident that the CrN/AlN multilayer with smaller modulation period exhibited better oxidation resistance.

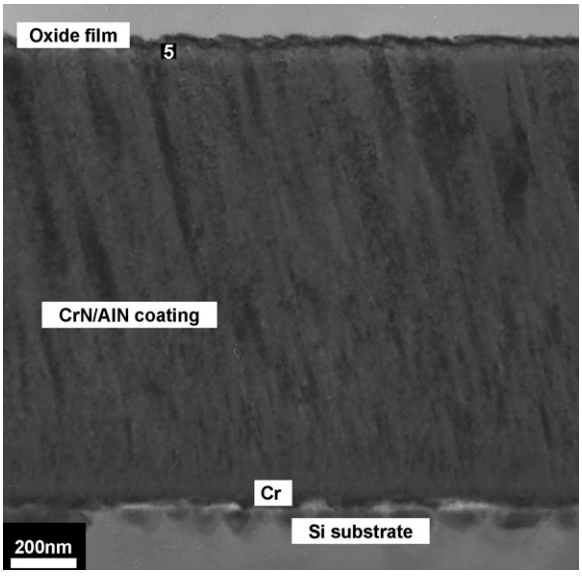

Fig. 3. X'TEM image of CrN/AlN multilayer coating with 4 nm annealed at 800 °C for 1 h.

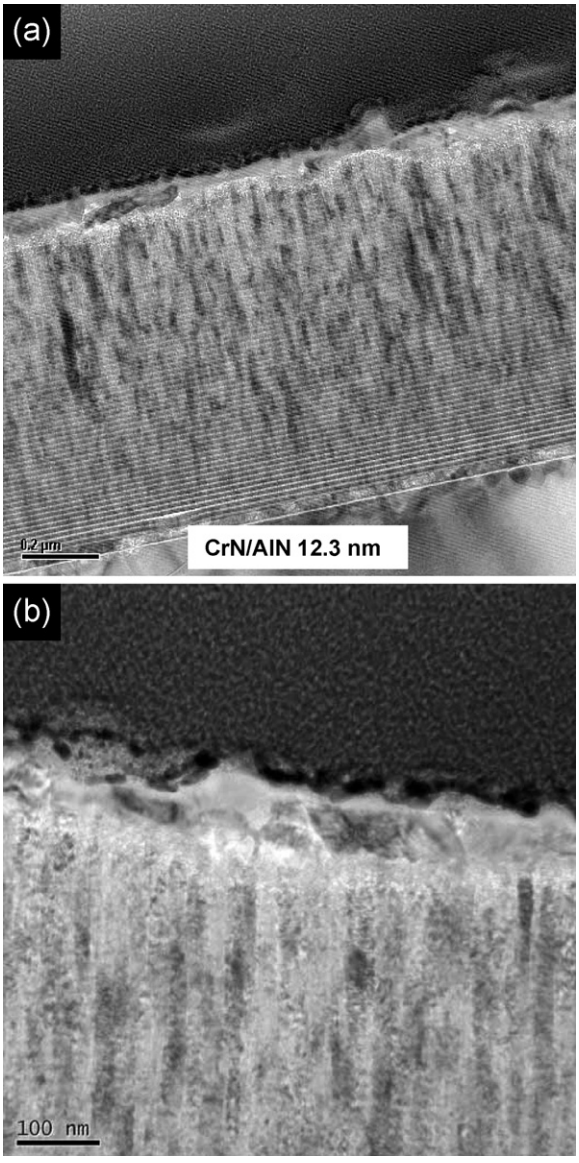

Fig. 4. (a) X'TEM image of CrN/AlN multilayer coating with 12.3 nm annealed at 800 °C for 16 h and (b) X'TEM image of interface between oxide and un-reacted CrN/AlN multilayer coating with 12.3 nm.

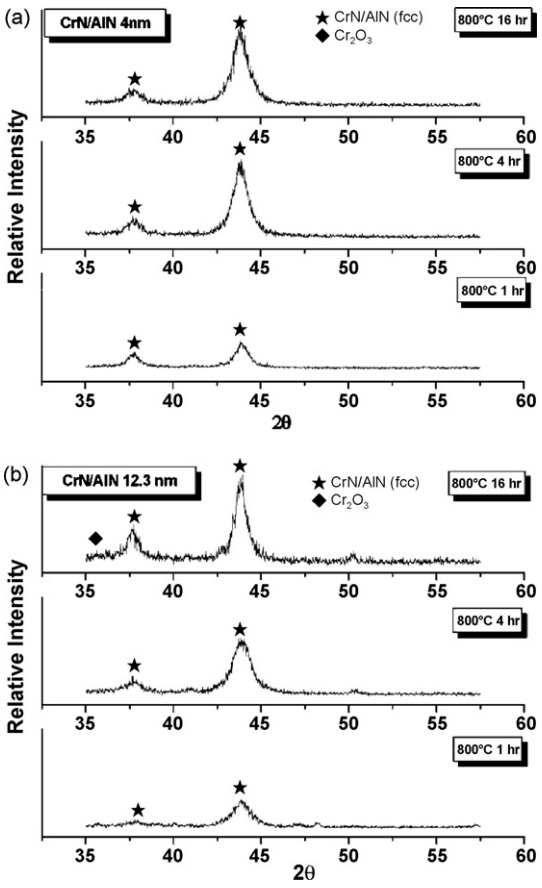

Fig. 5. X-ray diffraction patterns of (a) CrN/AlN with 4 nm, (b) CrN/AlN with 12.3 nm after heat treatment at 800 °C for 1, 4, and 16 h.

3.3. Microstructure analysis of the CrN/AlN multilayer coatings at 800 °C for 16 h

Fig. 4 indicates the microstructure of CrN/AlN multilayer coating with 12.3 nm after heat treatment at 800 °C for 16 h. The bilayer structure of CrN/AlN multilayer still existed. The oxide formed on the surface of CrN/AlN multilayer coating with 12.3 nm looks quite different as compared with that after heat treatment at 800 °C for 1 h in Fig. 2. The outmost Al-rich layer was almost crystallized with large grains. Besides, the interface between oxide and un-reacted CrN/AlN coating with 12.3 nm became abruptly rough, indicating that the oxidation on the surface was not uniform. The phase evolutions of CrN/AlN multilayer coatings after heat treatment at 800 °C for 1, 4, and 16 h, respectively, identified by X-ray diffraction pattern were illustrated in Fig. 5. The large crystalline grains formed in the CrN/AlN multilayer coating were attributed to the formation of Cr_2O_3.

The microstructure of CrN/AlN multilayer coating with 4 nm after heat treatment at 800 °C for 16 h is shown in Fig. 6. The cross-sectional CrN/AlN coating revealed dense columnar structure and bilayer structure still existed in the all un-reacted film even below the interface of oxidation zone. Besides, the oxide with thickness around 58 nm formed smoothly and uniformly on the surface of CrN/AlN multilayer coatings with 4 nm, which was much different as compared to that in the film with 12.3 nm. The phase in the CrN/AlN multilayer coating identified by XRD shows only f.c.c. CrN/AlN multilayer coating and no other peaks are found, implying that the oxide is amorphous, which is consistent with that observed from TEM.

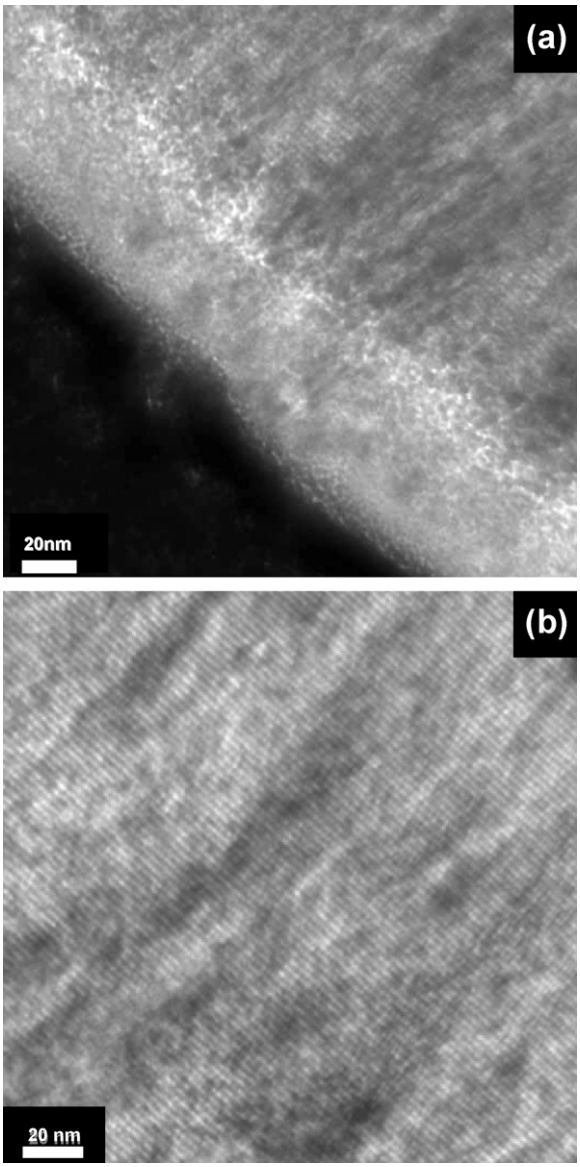

Fig. 6. X'TEM image of CrN/AlN multilayer coating with 4 nm annealed at 800 °C for 16 h. (a) Surface oxide and (b) multilayer film.

3.4. Microstructure analysis of the CrN/AlN multilayer coatings at 950 °C for 1 h

Fig. 7 displays the X'TEM image of the CrN/AlN multilayer coating with 12.3 nm at 950 °C for 1 h. It appeared that bilayer structure still prevailed even below the oxide film on the basis of the bright field image in Fig. 7(a). This phenomenon confirmed that the CrN/AlN multilayer exhibited excellent thermal stability at elevated temperatures and the bilayer structure retained. The oxide appearance formed on the CrN/AlN multilayer became similar as compared to that at 800 °C for 16 h. Two oxide layers were observed, including thick crystalline layer, and thin nano-crystalline films. The thick crystalline grains over 100 nm identified by SAED and EDS was Cr-rich $(Al_xCr_{1-x})_2O_3$, in which the topmost Al-rich oxide could not impede the outward diffusion of Cr to the air exposed surface in the CrN/AlN multilayer coating with 12.3 nm.

On the contrary, the microstructure of CrN/AlN multilayer coating with 4 nm after heat treatment at 950 °C for 1 h is shown in Fig. 8. The oxide interface remained smoothly and the oxide with

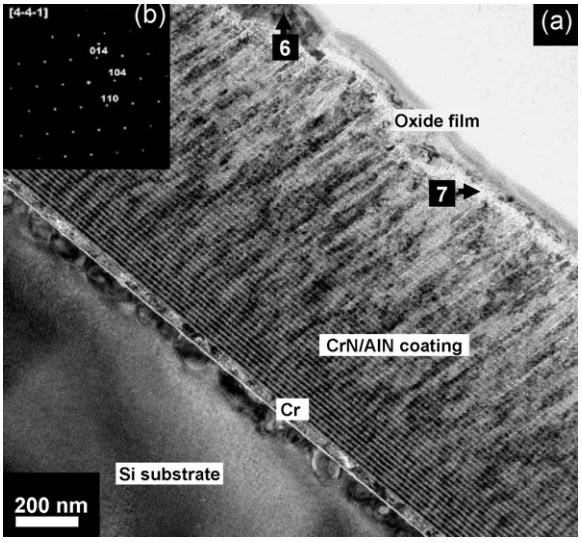

Fig. 7. (a) X'TEM image of CrN/AlN multilayer coating with 12.3 nm annealed at 950 °C for 1 h and (b) SAED pattern of crystalline oxide in point 6.

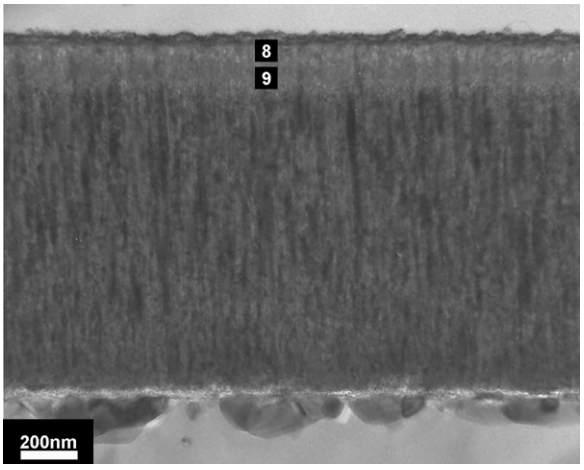

Fig. 8. X'TEM image of CrN/AlN multilayer coating with 4 nm annealed at 950 °C for 1 h.

thickness around 170 nm identified by TEM equipped with EDX is Al-rich oxide without crystallization.

The interface between un-reacted film and mixed nano-crystalline oxide in the CrN/AlN multilayer coating with 12.3 nm became complicated after heat treatment at 950 °C for 1 h and 800 °C for 16 h, which was much different as compared to that with 4 nm. It is suggested that the columnar structure of the nitride coating would provide pathway for diffusing species, which would accelerate oxidation reactions at identical temperatures. The multilayer coatings which exhibited the specific coherent interface vertical to the columnar structure acquired additional barrier layer for diffusion species and therefore displayed favorable anti-oxidation resistance, which was also evidenced in the TiN/AlN multilayer coatings with different modulation periods [22].

When oxidation occurred, the diffusion species in the same thickness with relatively large number of interfaces would suffer from more obstacles. For CrN/AlN multilayer coating with 12.3 nm, the less oxidized resistant Cr would easily gather together and formed crystalline Cr-rich $(Al_xCr_{1-x})_2O_3$ grains in spite of the protection of amorphous Al-rich $(Al_xCr_{1-x})_2O_3$. After heat treatment at identical temperatures for a period of time, the crystalline grains would merge together and grow rapidly. In contrast, for the multilayer coating with small modulation period, the oxide formed on the surface included only one Al-rich $(Al_xCr_{1-x})_2O_3$ and no crystallization occurred due to much complicated diffusion behaviors. Furthermore, it is believed from the Al_2O_3–Cr_2O_3 phase diagram that the solid solution between Al_2O_3 and Cr_2O_3 at elevated temperatures would also restrict the nucleation and grain growth of the oxides.

4. Conclusions

The microstructure evolutions of the CrN/AlN multilayer coating fabricated by the RF magnetron sputtering technique were analyzed systematically after heat treatment at 800, and 950 °C in air environment. Three distinct regions were found on the CrN/AlN multilayer coating with 12.3 nm at 800 °C for 1 h. (1) Al-rich $(Al_xCr_{1-x})_2O_3$ formed on the topmost layer and protected the unreacted film from oxidation; (2) spherical nano-voids embedded underneath the Al-rich oxide layer caused by the fast diffusion of atom species; (3) dense and mixed amorphous or nano-crystalline film covered the un-created CrN/AlN multilayer coating. Abruptly rough interface was also detected due to the non-uniform oxidation caused by the grain growth of the surface oxide after heat treatment at 800 °C for 16 h and at 950 °C for 1 h. On the contrary, the CrN/AlN multilayer coating with 4 nm exhibited superior oxidation resistance resulted from the dense amorphous Al-rich oxide protection even annealed at 800 °C for 16 h and at 950 °C for 1 h. It is believed that the specific interfaces between two nitrides layers also played an important role in the oxidation resistance at elevated temperatures.

Acknowledgment

Financial support from the National Science Council, Taiwan, under Contract No. NSC 96-2221-E-007-093 is appreciated.

References

[1] U. Helmersson, S. Todorova, S.A. Barnett, J.E. Sundgren, L.C. Markert, J.E. Greene, J. Appl. Phys. 62 (1987) 481.
[2] M.S. Wong, G.Y. Hsiao, S.Y. Yang, Surf. Coat. Technol. 133–134 (2000) 160.
[3] D.C. Cameron, R. Aimo, Z.H. Wang, K.A. Pischow, Surf. Coat. Technol. 142–144 (2001) 567.
[4] H.Y. Lee, J.G. Han, S.H. Baeg, S.H. Yang, Thin Solid Films 420–421 (2002) 414.
[5] F.B. Wu, S.K. Tien, J.G. Duh, Surf. Coat. Technol. 200 (2005) 1514.
[6] Y.Z. Tsai, J.G. Duh, Surf. Coat. Technol. 200 (2006) 1683.
[7] C. Mendibide, J. Fontaine, P. Steyer, C. Esnouf, Tribol. Lett. 17 (2004) 779.
[8] M. Setoyama, M. Irie, H. Ohara, Y. Takeda, T. Nomura, N. Kitagawa, Thin Solid Films 341 (1999) 126.
[9] H.C. Barshilia, K.S. Rajam, Surf. Coat. Technol. 183 (2004) 174.
[10] D.G. Kim, T.Y. Seong, Y.J. Baik, Surf. Coat. Technol. 153 (2002) 79.
[11] Q. Yang, L.R. Zhao, J. Vac. Sci. Technol. A 21 (2003) 558.
[12] X.T. Zeng, S. Zhang, C.Q. Sun, Y.C. Liu, Thin Solid Films 424 (2003) 99.
[13] H.C. Barshilia, M.S. Prakash, A. Jain, K.S. Rajam, Vacuum 77 (2005) 169.
[14] H.C. Barshilia, A. Jain, K.S. Rajam, Vacuum 74 (2004) 241.
[15] M. Kawate, A.K. Hashimoto, T. Suzuki, Surf. Coat. Technol. 165 (2003) 163.
[16] G.S. Kim, S.Y. Lee, J.H. Hahn, S.Y. Lee, Surf. Coat. Technol. 171 (2003) 91.
[17] J.K. Park, Y.J. Baik, Surf. Coat. Technol. 200 (2005) 1519.
[18] S.K. Tien, J.G. Duh, Thin Solid Films 494 (2006) 173.
[19] D.B. Lee, Surf. Coat. Technol. 173 (2003) 81.
[20] H. Ichimura, A. Kawana, J. Mater. Res. 8 (1993) 1093.
[21] H. Ichimura, A. Kawana, J. Mater. Res. 9 (1994) 151.
[22] D.G. Kim, T.Y. Seong, Y.J. Baik, Surf. Coat. Technol. 397 (2001) 203.